International Journal of Architectural, Civil and Construction Sciences
ISSN: 2415-1734
Vol:8, No:6, 2014

Study the Behavior of Different Composite Short Columns (DST) with Prismatic Sections under Bending Load

V. Sadeghi Balkanlou, M. Reza Bagerzadeh Karimi, A. Hasanbakloo, B. Bagheri Azar

***Abstract*—**In this paper, the behavior of different types of DST columns has been studied under bending load. Briefly, composite columns consist of an internal carbon steel tube and an external stainless steel wall that the between the walls are filled with concrete. Composite columns are expected to combine the advantages of all three materials and have the advantage of high flexural stiffness of CFDST columns. In this research, ABAQUS software is used for finite element analysis then the results of ultimate strength of the composite sections are illustrated.

***Keywords*—**DST, Stainless steel, carbon steel, ABAQUS, Straigh Columns, Tapered Columns.

I. Introduction

IN recent decades, several tests were conducted on composite columns; Han has done a research on the behavior of composite CFT columns under pure torsion. Han in this research examined the performance and square steel tubular columns filled with concrete under pure torsion using the ABAQUS software. The finite element method (FEA) was used to assess the impact of important parameters that determine the ultimate tensional strength of composite sections. Han found that steel pipe plays an important role in the tensional resistance of composite columns which are square or circular, and the composite columns show a good Stability and plastic behaviour under torsion [1]-[6].

Elremaily performed a Research on composite columns under earthquake loads [7]. He found that CFT columns under seismic loads, show very high levels of ductility and energy dissipation. It was also observed that the test samples maintained the flexural capacity until the test to be concluded.

Oyawa has done tests on composite steel columns filled with polymer concrete under axial load [8]. He found that polymer concrete has high tensile adhesion capacity, less weight, less shrinkage, reversible and ductility than conventional concrete. The polymer concrete has a high resistance against chemical and physical blows.

Recent laboratory researches in Japan affirmed the growing demand and strong potential use in Japan (CFDT) in the construction of highways and airways free, especially as a middle ground lift bridges (with a height of more than m 100) in remote areas of steep mountains. The good damping characteristics and relatively light weight are the main reasons to use (CFDT) for dynamically sensitive structures.

Yagishita and colleagues [9] have done six tests on tubular steel columns CFDT soft thin circular diameter thickness ratio D/t = 130-250 and filled with normal concrete collar. They concluded that the multilayer columns had a better performance than CFT members in terms of the characteristics of strength, ductility and energy absorption under lateral cyclic loading and constant axial force, respectively.

Nakanashi and colleagues [10] conducted ten tests of periodic launches on pillars of CFDT and CFT, Their goal was to propose a new design for the central base of bridge to not be damaged after intense earthquakes (0.8g), but a little force was transmitted to the foundations. The outer casing was made from Composite cans (f_y = 315 MPa) with a width-to-thickness ratio B/t = 14 ~ 66. Circular tube is made of plastic or metal lining. Light concrete with compressive strength f_c = 13 MPa was used to fill the cylinder to reduce loads. They compared the periodic remnants for CFDT with rigid and prefabricated containers and CFT. Their conclusions are similar to the conclusions of Yagishita and colleagues. Where CFDT improved the behavior of remnants and the most ductile member was found compared to most other types.

Some studies have been done on elliptical hollow steel sections filled with concrete. A series of short columns of steel - concrete - FRPDST have been studied by Tang [11]-[13].

Results of tests of short CFT columns showed that filling Steel pipe with concrete increases the strength, ductility and energy absorption higher than the diameter of the hollow tube thickness (D/t). This is due to the confining the concrete core and steel tube wall to restrain local buckling. If the module level increases using multi-layer technique tubular steel columns and circle centre filled with towering concrete materials (CFDT), In this case, the overall Sustainability of the members is greater when compared with CFT [14], [15].

The advantages of making multilayer CFDT when compared with CFT columns are as following:

High flexural stiffness, avoiding instability under external pressure, interactions of three components of (outer steel pipe, concrete, inner steel pipe) results in a good position stability, increased Section modulus, improved overall stability, better seismic strengthening, better coupled with a circular steel

M. Reza Bagerzadeh Karimi* is with the Young Researchers and Elite Club, Tabriz Branch, Islamic Azad University, Tabriz, Iran (Corresponding author to provide phone: +989141060397; e-mail: MRBKarimi@yrct.ir, MRBKarimi@gmail.com).

A. Hasanbakloo is with the Department of Civil Engineering, Islamic Azad University, Maragheh Branch, Iran.

V. Sadeghi Balkanlou and B. Bagheri Azar are with the Young Researchers and Elite Club, Tabriz Branch, Islamic Azad University, Tabriz, Iran.

columns, lighter weight, and performance characteristics of a good attenuation. Multi-layer construction technique uses a variety of filler materials. For example it is used as epoxy filler for pressure tanks, concrete water tanks, deep, tunnel construction, manufacturing base in the middle of the bridge in Japan, seismic strengthening and foundation piles.

It is believed that the excellent performance of a composite member will be shown than a simple set of concrete and normal pipes. Due to the high cost, stainless was not commonly used as a material of construction in the past. However, after the developments over the past decade, both in terms of material availability and terms of durability, sometimes it is suggested that the main structural material of stainless steel, can be used. The studied parameters for composite column samples are considered as follows:

Type of column: Straight and muscular. The tapered angle for DST columns is designed as 1 degree to refer to the Structural muscular columns.

Type of cross-section: Circular, square, rectangular, round or elliptical corners.

In this study, firstly the anchor of DST composite short column for the displacement applied to the free end of the column was calculated by the software and the ultimate flexural capacity is determined. Displacement applied to the free end of the column is 30 mm as shown in Fig. 1.

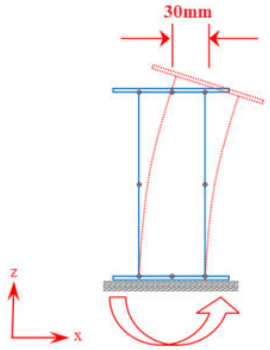

Fig. 1 Applying displacement to the free end of the column and determining the bending moment at the foot of the column

II. The Examples Presented in the Analysis in Abaqus Software

A collection contains 24 specimens were tested in this program, which includes 16 DST Stainless Steel - Concrete - carbon steel columns and 8 samples with empty sections. Fig. 2 offers a schematic view of the test samples.

Test parameters for composite column samples include:

Type of column: Straight and tapered. The tapered angle for DST columns is designed as 1 degree to refer to the Structural muscular columns.

Type of cross-section: Circular, square, rectangular, round or elliptical corners, as is shown in Fig. 3.

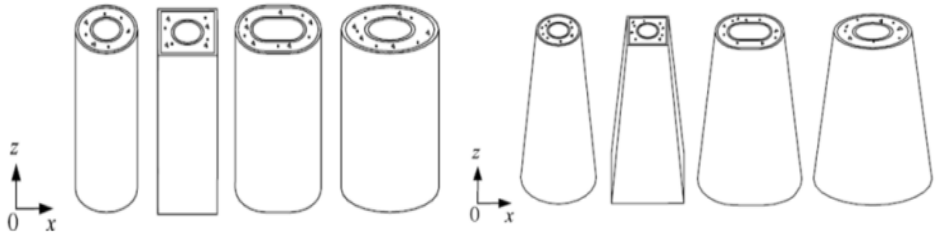

(a) Straight Column (b) Tapered Column

Fig. 2 Different DST column types used in the bending capacity test

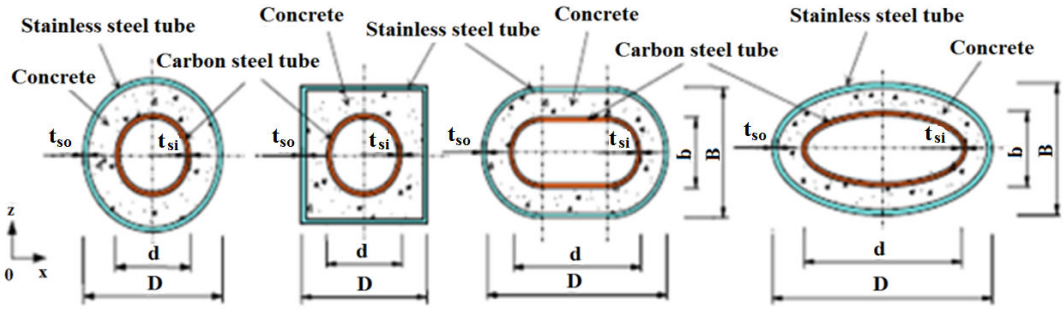

Fig. 3 Different types of cross section for DST columns used in the bending test

The ratio of DST composite cross-section hole and x can be presented as follows:

$$x = \frac{d}{D-2t_{so}} \quad (1)$$

For circular and square sections

$$x = \sqrt{\frac{bd}{(B-2t_{so})(D-2t_{so})}} \quad (2)$$

For rectangular sections

A summary of the sample data is provided in Table I.

The following procedure is used for naming samples:

The main character of "T" represents the muscular columns. The directions of x, y, z are shown in Figs. 2 and 3, if (not written) remain white, they represent straight columns.

Characters of C, S, R, E represent the circular cross section, square, rectangular, round or elliptical corners, respectively.

The last character of H (if any) indicates the empty column without filling concrete.

The first figures represent the different groups of the same type of column.

The second figures represent a different sample of the same groups.

Both stainless and carbon steel pipes have been provided by steel plates. Steel plates are bent into two sections or half-oval for circular and elliptical cross sections and are butt-welded together in order to achieve a circular or elliptical section.

For a square cross section, 4 parts of steel plate are butt-welded together to form a square cross section and for rounded corners of the rectangular cross section, 2 sections of steel plates are bent into circular sections and are butt-welded together in order to obtain the desired level.

Self-compacted concrete (scc) is designed to place the distance between the outer stainless steel pipe and carbon steel inner tube and then the DST samples are placed vertically to test. During the curing of the concrete, a very small amount of longitudinal shrinkage of the sample occurs. Then a high-strength concrete is used to fill the gap length in order to align the concrete surface with a steel pipe. To ensure the complete transfer of vertical load on the composite section, two carbon-based steel plates with a thickness of 20cm are butt-welded to the inner and outer tubes at the ends of each DST sample and one plate is welded before pouring concrete and the other one is welded before the test.

TABLE I
SUMMARY OF DATA SAMPLES

Series	section	No	Specimen label	Outer tube D × B × tso		Inner tube d × b × tsi		x
				Section A-A	Section B-B	Section A-A	Section B-B	
		1	C1-1	220×220×3.62	220×220×3.62	159×159×3.72	159×159×3.72	0.75
		2	C2-2	220×220×3.62	220×220×3.62	106×106×3.72	106×106×3.72	0.5
		3	CH1-1	220×220×3.62	220×220×3.62	159×159×3.72	159×159×3.72	0.75
		4	S1-1	220×220×3.62	220×220×3.62	159×159×3.72	159×159×3.72	0.75
		5	S2-2	220×220×3.62	220×220×3.62	106×106×3.72	106×106×3.72	0.5
		6	SH1-1	220×220×3.62	220×220×3.62	159×159×3.72	159×159×3.72	0.75
		7	R1-1	240×160×3.62	240×160×3.62	186×106×3.72	186×106×3.72	0.75
		8	R2-2	240×160×3.62	240×160×3.62	142×62×3.72	142×62×3.72	0.5
		9	RH1-1	240×160×3.62	240×160×3.62	186×106×3.72	186×106×3.72	0.75
		10	E1-1	240×160×3.62	240×160×3.62	186×106×3.72	186×106×3.72	0.75
		11	E2-2	240×160×3.62	240×160×3.62	142×62×3.72	142×62×3.72	0.5
		12	EH1-1	240×160×3.62	240×160×3.62	186×106×3.72	186×106×3.72	0.75
		13	TC1-1	197×197×3.62	220×220×3.62	136×136×3.72	159×159×3.72	0.75
		14	TC2-2	197×197×3.62	220×220×3.62	83 × 83 × 3.72	106×106×3.72	0.5
		15	TCH1-1	197×197×3.62	220×220×3.62	136×136×3.72	159×159×3.72	0.75
		16	TS1-1	197×197×3.62	220×220×3.62	136×136×3.72	159×159×3.72	0.75
		17	TS2-2	197×197×3.62	220×220×3.62	83 × 83 × 3.72	106×106×3.72	0.5
		18	TSH1-1	197×197×3.62	220×220×3.62	136×136×3.72	159×159×3.72	0.75
		19	TR1-1	215×135×3.62	240×160×3.62	161×81×3.72	186×106×3.72	0.75
		20	TR2-2	215×135×3.62	240×160×3.62	117×37×3.72	142×62×3.72	0.5
		21	TRH1-1	215×135×3.62	240×160×3.62	161×81×3.72	186×106×3.72	0.75
		22	TE1-1	215×135×3.62	240×160×3.62	161×81×3.72	186×106×3.72	0.75
		23	TE2-2	215×135×3.62	240×160×3.62	117×37×3.72	142×62×3.72	0.5
		24	TEH1-1	215×135×3.62	240×160×3.62	161×81×3.72	186×106×3.72	0.75

III. MATERIALS PROPERTIES

A. Steel:

A stainless steel and carbon steel are used in order to make the inner and outer tubes. Standard tensile tests are done to measure material properties of stainless steel and carbon. The average measured yield strength (f_y), ultimate strength (f_u), modulus of elasticity (E_s) and Poisson's ratio are listed in Table II.

TABLE II
PROPERTIES OF MATERIALS USED IN THE STEEL

Type	Thickness (mm)	f_y (MPa)	f_u (MPa)	E_s (N/mm^2)	y_s
Carbon steel	3.72	380.6	519.1	1.92x105	0.282
Stainless Steel	3.62	319.6	626.5	2.01x105	0.286

B. Concrete:

A mixture of Scc with a cubic sample compressive strength of 60 Mpa is designed approximately in 28 days. Elastic modulus scc (E_s) is equal to 33,000 N per square millimeter. Scc combination of properties is as following: Cement: 440 kg/m^3, slag, iron maidens: 143 kg/m^3 of water: 194 kg/m^3, 683 kg/m^3 of sand, coarse aggregate: 855 kg/m^3, a lubricant (HRWR): 5.83 kg/m^3. In Figs. 4 (a) and (b) show the stress - strain of concrete in compression and tension, respectively.

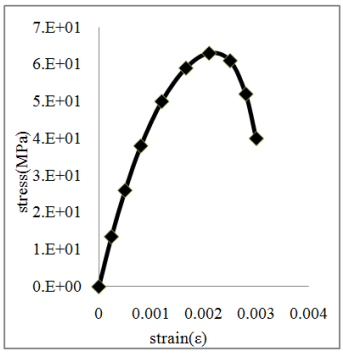

(a)

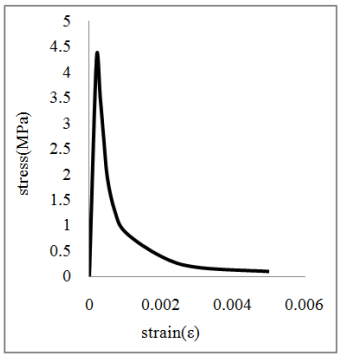

(b)

Fig. 4 (a) diagram of the stress - strain of concrete in compression, (b) diagram of the stress - strain of concrete in tension

IV. PRESENTING THE ABAQUS SOFTWARE ANALYSIS RESULTS FOR BENDING

In Figs. 5 to 7 Von Mises stress distribution, amount and location of maximum stress for column C1 -1 is shown in the last stage of loading under moment in ABAQUS. Moment-displacement axis from the ABAQUS analysis is shown for the intended column under bending moment about the y-y axis.

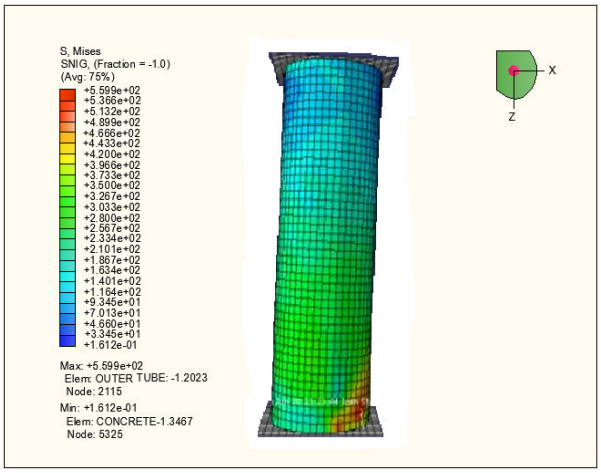

Fig. 5 Schematic view of Von Mises stress distribution in column C1-1 under bending moment in program

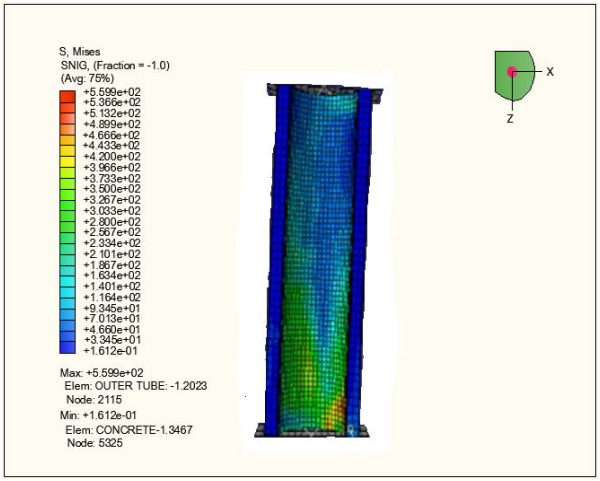

Fig. 6 Schematic view of Von Mises stress distribution in vertical incision of column C1-1 under bending moment

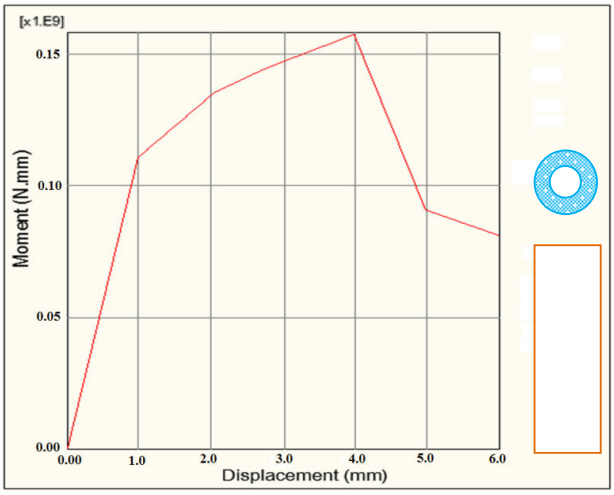

Fig. 7 Bending moment axis at the foot of the column against the displacement applied to the free end of the column in ABAQUS for column C1-1 (x=0.75)

V. Analysis of Results and Comparison of Graphs for Bending

The results of numerical analysis for DST composite short columns for bending are listed in Table III. In the first and second columns of the table, the column type and section are shown and in the third and fourth columns of the table the column name and values for the ratio of hole are illustrated and finally the last column gives the ultimate flexural capacity of DST composite short column, respectively.

As it can be seen, bending moment graph against the free end displacement for straight columns with circular section modeled by ABAQUS software are plotted in Fig. 8.

Finally, the ultimate flexural capacity of DST short columns for both straight and tapered series for different sections are shown in Figs. 10 and 12.

TABLE III
Determining the Ultimate Capacity of DST Short Columns under Bending

Series	section	Spe. label	χ	M_{ue}(KN.m)
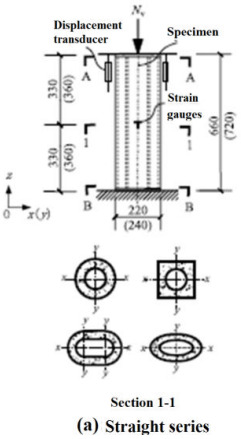 (a) Straight series		C1-1	0.75	1.58E+02
		C2-2	0.50	1.41E+02
		CH1-1	0.75	9.53E+01
		S1-1	0.75	1.62E+02
		S2-2	0.50	1.83E+02
		SH1-1	0.75	1.10E+02
		R1-1	0.75	1.56E+02
		R2-2	0.50	1.45E+02
		RH1-1	0.75	1.05E+02
	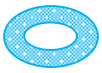	E1-1	0.75	1.42E+02
		E2-2	0.50	1.33E+02
		EH1-1	0.75	1.23E+02
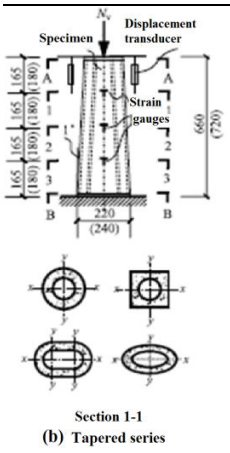 (b) Tapered series	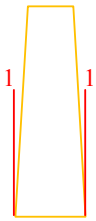	TC1-1	0.75	1.52E+02
		TC2-2	0.50	1.35E+02
		TCH1-1	0.75	9.47E+01
		TS1-1	0.75	2.03E+02
		TS2-2	0.50	1.87E+02
		TSH1-1	0.75	1.07E+02
		TR1-1	0.75	1.57E+02
		TR2-2	0.50	1.44E+02
		TRH1-1	0.75	1.04E+02
		TE1-1	0.75	1.43E+02
		TE2-2	0.50	1.33E+02
		TEH1-1	0.75	9.54E+01

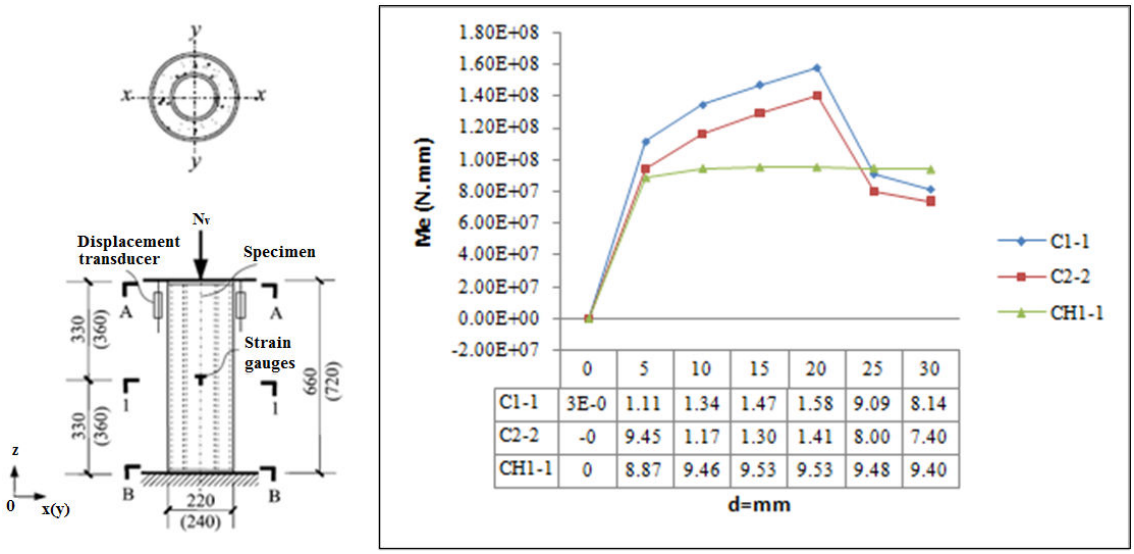

	0	5	10	15	20	25	30
C1-1	3E-0	1.11	1.34	1.47	1.58	9.09	8.14
C2-2	-0	9.45	1.17	1.30	1.41	8.00	7.40
CH1-1	0	8.87	9.46	9.53	9.53	9.48	9.40

Fig. 8 Moment-displacement curve for columns CH1-1, C2-2, C1-1

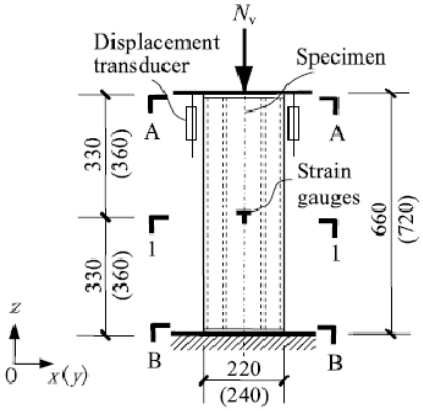

Fig. 9 Straight series details

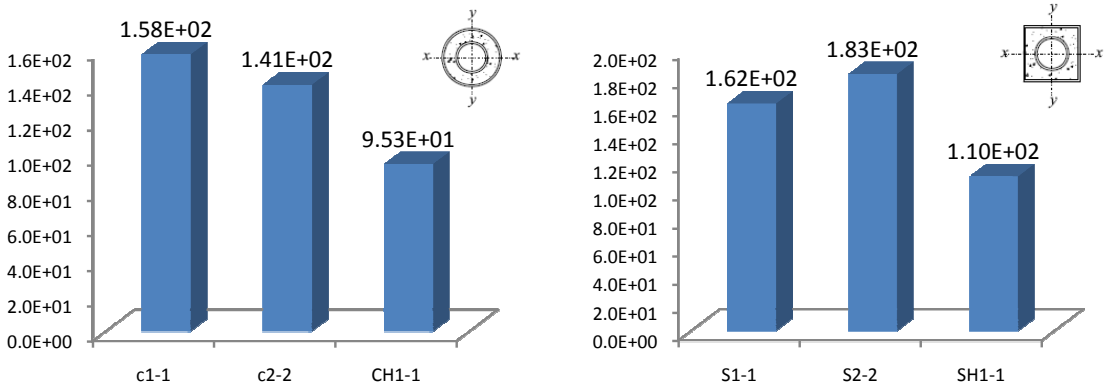

(a) **(b)**

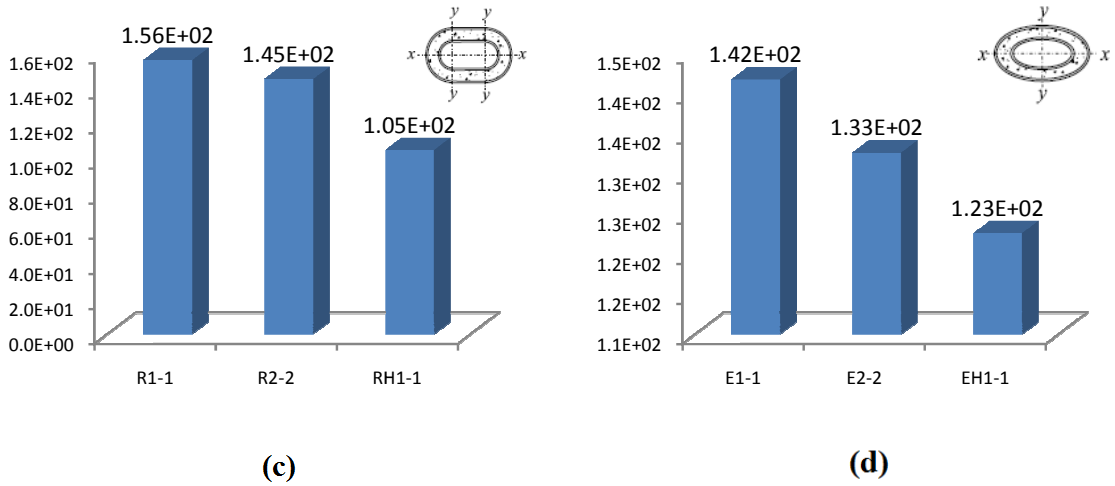

Fig. 10 Column charts for flexural capacity of DST columns for straight series (kN.m)

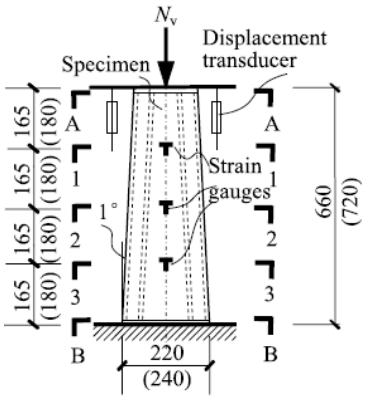

Fig. 11 Tapered series details

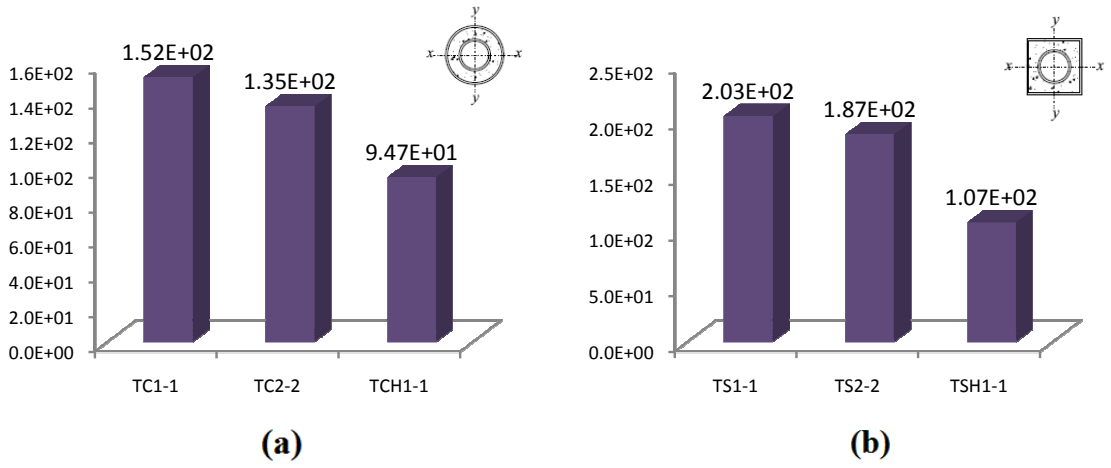

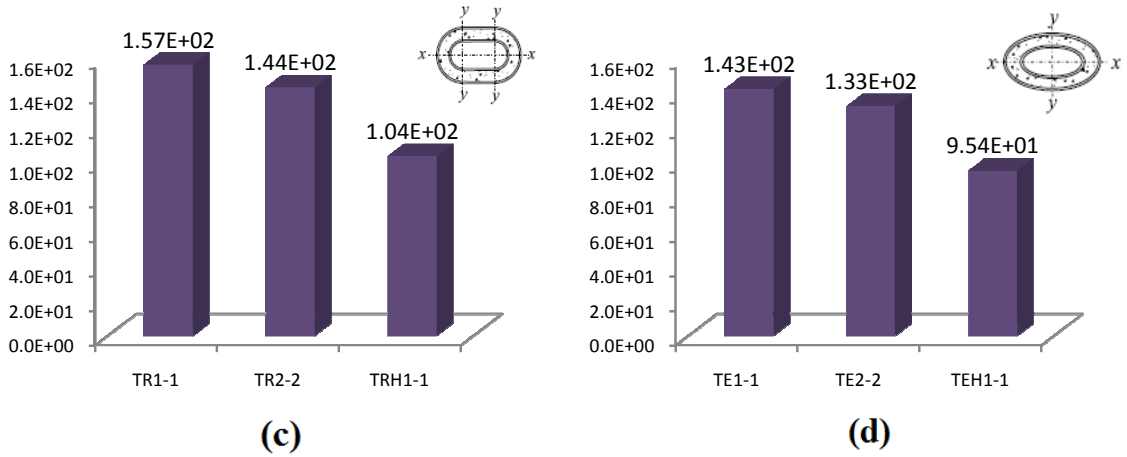

Fig. 12 Column charts for flexural capacity of DST columns for tapered series (kN.m)

To verify the performance of DST columns having ultimate flexural capacity for the columns of straight and tapered series and also verify the ultimate flexural capacity of DST filled columns with sandwich concrete and hollow have been illustrated in Figs. 13 and 14, respectively.

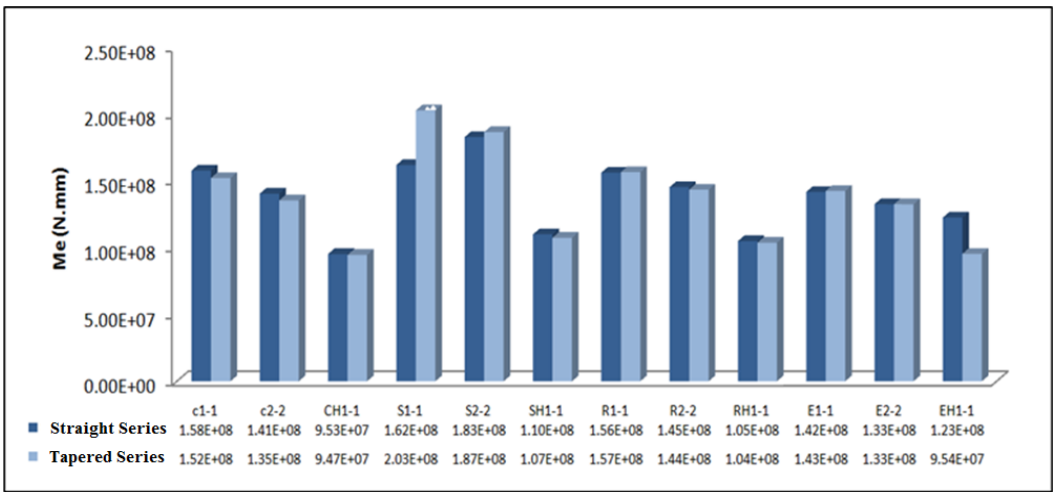

Fig. 13 Flexural capacity of columns for both straight and tapered series

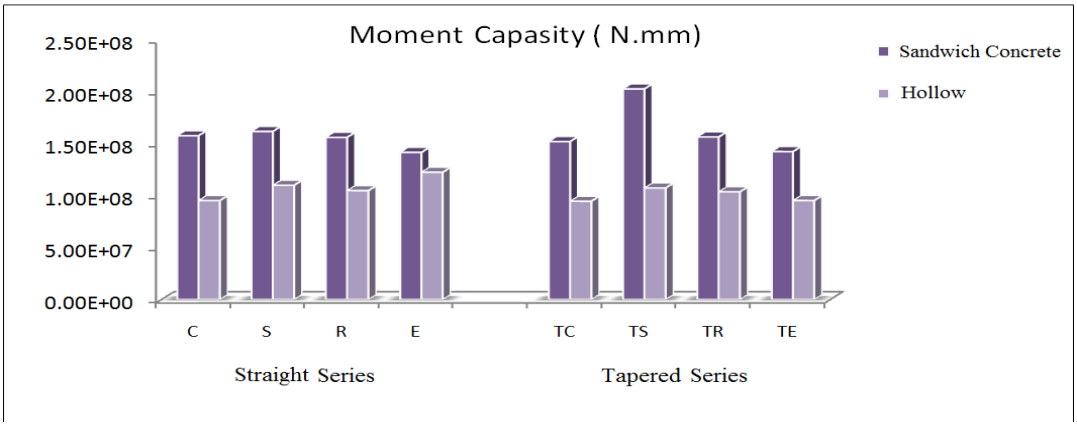

Fig. 14 Flexural capacity of DST filled columns with sandwich concrete and hollow both for straight and tapered series

V. Conclusion

In this study, the performance of DST columns with straight and tapered section was evaluated under the force of bending moment. The results are as following:

- The bending strength of transverse sections (M_{ue}) and flexural stiffness of straight column increases with an increase of the ratio of hole (X).
- Aside from the square section that increases with decreasing the ratio of hole, and increases markedly by filling the sandwiched concrete.
- The bending strength of transverse sections (M_{ue}) and flexural stiffness of tapered column increases with an increase of the ratio of the hole (X) and obviously, increases by filling the sandwiched concrete.
- Among the short columns (the ratio of larger dimension of section to the column height equals to 1.3) DST hollow columns with straight series and the hole ratio (X) is equal to 0.75, the elliptical section has the highest flexural capacity and among the DST hollow columns with tapered series, the square section has the highest flexural capacity in bending around the strong-axis of the column.
- For DST short columns filled with concrete with hole ratio, equal to 0.75, 0.50, respectively, the square section has the highest flexural capacity for both straight and tapered columns in bending around the strong-axis of the column.
- The bending strength of transverse sections (M_{ue}) shows the DST columns filled with concrete and DST hollow columns. It can be observed that the resistance of composite columns increases due to the filling of the sandwich concrete. For straight members, the flexural strength of DST circular, square, rectangular, round or elliptical columns filled with concrete is 1.15, 1.49, 1.47, and 1.66 equal to hollow pipes.
- For short tapered columns, the flexural strength of DST circular, square, rectangular, round or elliptical members filled with concrete is 1.50, 1.51, 1.90, and 1.61 equal to hollow pipes.

References

[1] Schneider SP. Axially loaded concrete-filled steel tubes. Journal of Structural Engineering, ASCE 1998; 124(10):1125–38.
[2] Han LH. Tests on stub columns of concrete-filled RHS sections. Journal of Constructional Steel Research 2002; 58(3):353–72.
[3] Zhao XL, Grzebieta RH, Elchalakani M. Tests of concrete-filled double-skin CHS composite stub columns. Steel and Composite Structures—An International Journal 2002; 2(2):129–42.
[4] Han LH, Tao Z, Huang H, Zhao XL. Concrete-filled double-skin (SHS outer and CHS inner) steel tubular beam–columns. Thin-Walled Structures 2004; 42(9):1329–55.
[5] Zhao XL, Han LH. Double-skin composite construction. Progress in Structural Engineering and Materials 2006; 8(3):93–102.
[6] Huang H, Han LH, Tao Z, Zhao XL. Analytical behaviour of concrete-filled double-skin steel tubular (CFDST) stub columns. Journal of Constructional Steel Research 2010; 66(4):542–55.
[7] Dabaon MA, El-Khoriby S, El-Boghdadi MH. Confinement effect of stiffened and unstiffened concrete-filled stainless steel tubular stub columns. Journal of Constructional Steel Research 2009; 65(8):1846–54.
[8] Lam D, Gardner L. Structural design of stainless steel concrete-filled columns. Journal of Constructional Steel Research 2008; 64(11):1275–82.
[9] Yang H, Lam D, Gardner L. Testing and analysis of concrete-filled elliptical hollow sections. Engineering Structures 2008; 30(12):3771–81.
[10] Zhao XL, Packer JA. Tests and design of concrete-filled elliptical hollow section stub columns. Thin-Walled Structures 2009; 47(6):617–28.
[11] Lam D, Dai X. Numerical modelling of the axial compressive behavior of short concrete-filled elliptical steel columns. Journal of Constructional Steel Research 2010;66(7):931–42.
[12] Teng JG, Yu T, Wong YL, Dong SL. Hybrid FRP–concrete–steel tubular columns: concept and behavior. Construction and Building Materials 2007; 21(4): 846–54.
[13] Dabaon MA, El-Boghdadi MH, Hassanein MF. Experimental investigation on concrete-filled stainless steel stiffened tubular stub columns. Engineering Structures 2009; 31(2):300–7.
[14] Tao Z, Uy B, Liao FY, Han LH. Finite element modelling of concrete-filled square stainless steel tubular stub columns under axial compression. In: Proceedings of the 5th international symposium on steel structures. 2009, p. 87
[15] Han LH, Ren QX, Li W. Tests on inclined, tapered and STS concrete-filled steel tubular (CFST) stub columns. Journal of Constructional Steel Research 2010; 66(10):1186– 95.